energies

Article

A RBFNN & GACMOO-Based Working State Optimization Control Study on Heavy-Duty Diesel Engine Working in Plateau Environment

Yi Dong [1], Jianmin Liu [1], Yanbin Liu [1,*], Xinyong Qiao [1], Xiaoming Zhang [1], Ying Jin [1], Shaoliang Zhang [1], Tianqi Wang [1] and Qi Kang [2]

1 Vehicle Engineering Department, Army Academy of Armored Forces, Beijing 100072, China; 13391567396@163.com (Y.D.); Liujianmin@163.com (J.L.); aafeqxy@sina.com (X.Q.); true@163.com (X.Z.); Jinying@163.com (Y.J.); Zhangsl@163.com (S.Z.); Wangtianqi@163.com (T.W.)
2 China Satellite Maritime Tracking and Controlling Department, Wuxi 214431, China; kangqi@163.com
* Correspondence: yanbin.liu@xecaturbo.cn; Tel.: +86-185-1458-6180

Received: 15 December 2019; Accepted: 2 January 2020; Published: 6 January 2020

Abstract: In order to solve issues concerning performance induction and in-cylinder heat accumulation of a certain heavy-duty diesel engine in a plateau environment, working state parameters and performance indexes of diesel engine are calculated and optimized using the method of artificial neural network and genetic algorithm cycle multi-objective optimization. First, with an established diesel engine simulation model and an orthogonal experimental method, the influence rule of five performance indexes affected by five working state parameters are calculated and analyzed. Results indicate the first four of five working state parameters have a more prominent influence on those five performance indexes. Subsequently, further calculation generates correspondences among four working state parameters and five performance indexes with the method of radial basis function neural network. The predicted value of the trained neural network matches well with the original one. The approach can fulfill serialization of discrete working state parameters and performance indexes to facilitate subsequent analysis and optimization. Next, we came up with a new algorithm named RBFNN & GACMOO, which can calculate the optimal working state parameters and the corresponding performance indexes of the diesel engine working at 3700 m altitude. At last, the bench test of the diesel engine in a plateau environment is employed to verify accuracy of the optimized results and the effectiveness of the algorithm. The research first combined the method of artificial neural network and genetic algorithm to specify the optimal working state parameters of the diesel engine at high altitudes by focusing on engine power, torque and heat dissipation, which is of great significance for improving both performance and working reliability of heavy-duty diesel engine working in plateau environment.

Keywords: diesel engine; plateau; radial basis function neural network; genetic algorithm; multi-objective optimization

1. Introduction

Compared with plain, plateau features lower atmospheric pressure and air density. Consequently, when working in a plateau environment, the diesel engine becomes troubled with such problems as excessively high exhaust temperature, black smoke, overheating key parts, power performance, and fuel economy reduction, which severely restrain performance of diesel engine, especially the heavy-duty ones. This also produces a serious adverse effect on national economy, industrial production at plateau. Since air in plateau environment remains thin, quantity of air entering cylinder reduces. Air pressure and density in combustion chamber are lowered when piston is compressed to top dead center (TDC), impairing both quality and temperature of air-fuel mixture so that a combustion lag or incomplete combustion appears. The final consequence is diesel engine fail to operate normally. In view of such phenomenon, it remains an important issue in this field to make a detailed study of matching and controlling strategies among intake, exhaust and oil supply in diesel engine working in plateau environment.

In view of dramatic performance reduction of diesel engine working in plateau environment, scholars have made a lot of useful explorations. Zhengxia Zhu et al., [1] optimized fuel-injection quantity under rated conditions in the plateau environment using a genetic algorithm with penalty function and diesel engine operation process simulation model, and their results indicate post-optimization power of engine rises by 22.7%, efficiency of engine rises by 6.4%. Huaiqing Zhong et al. [2] established operation simulation model of certain diesel engine through such software as BOOST, and verified the model with experimental data. Later, they proposed some plateau-specific optimizing and improving measures such as "replacing with mass flow supercharger", "raising compression ratio" and "enlarging fuel supply advance angle" on the basis of this simulation model. To cope with power performance reduction and combustion deterioration of certain heavy-duty diesel engine in plateau environment, Piqiang Tan et al., [3] experimented with combined parameters of different compression ratio, turbine ratio and oil atomizer nozzle diameter, and finally determined three optimal plans that could improve power, fuel economy, and emission performance of diesel engine working in plateau environment. Hong Zhang et al., [4] studied the performance of compressor of diesel engine working at plateau, they use the simulation model of diesel engine to calculate the effect of environment parameter and key parameter of compressor to the performance of compressor. At last, they obtained the key parameters that affect the compressor's performance the most. The results of their study can help to improve the performance reduction condition of compressor and engine working at plateau. Meng Xia et al., [5] using the genetic algorithm and GT-POWER simulation model to improve the performance of 6V diesel engine, which works at plateau, show that the fuel consumption deterioration is restricted minus 5% and the torque is increased by 9%. There are also other researches focusing on combustion [6], emission [7], blend oil [8], performance optimization [9], spray pattern [10] of diesel engine.

With the emerging of artificial intelligence (AI) and machine learning, many scholars have applied it to calculate, predict and optimize diesel engine's performance. In the hope of figuring out the optimum ratio of biodiesel, Ka In Wong et al., [11] created a simulation model of diesel engine using experimental data, extreme learning machine (ELM), and least squares support vector machine (LS-SVM), then they compared and analyzed the strengths and weaknesses of two algorithms (simulated annealing algorithm and particle swarm optimization algorithm) in finding the optimum biodiesel proportion using the simulation model. Jinxing Zhao et al., [12] computed and analyzed optimal fuel economy of an Atkinson cycle engine with approach of artificial neural network (ANN). Based on one-dimensional simulation model and genetic algorithm (GA), the author conducted an optimization study on fuel economy of diesel engine operating under part load. As such, parameters as inlet valve closing timing, exhaust valve opening timing, electronic throttle control part, electric spark timing and air-fuel ratio were optimized, and fuel economy of diesel engine got elevated by 7.67% after optimization. HeeCheong Yoo et al., [13] studied the effects of electric supercharger and exhaust gas recirculation to the emissions and fuel efficiency of the diesel engine; authors also used the method of design of experiment and plotted the response surface of the BSFC. At last, they get the optimal Pareto fronts. Marco Bietresato et al., [14] used the response surface methodology (RSM) to analyze the correspondence relationship between the performance of internal combustion engine and biofuel blends condition. According to the result, this method shows good prediction capabilities and blend composition can be applied to accurately predict the performance of the engine. Bahman Najafi et al. [15] used the intelligent artificial neural network and RSM to get the optimal fuel blend of the diesel engine, the calculation and experiment results show that optimum values of exergy and energy efficiencies are in the range of 25–30% of full load. There are also some other algorithms applied to this field, e.g., support vector machine (SVM) [16], artificial bee colony (ABC) [17], energy blockchain network (EBN) [18], Multiple Utility Problem Table (MUPT) [19], quasi-optimal (QO) [20] algorithm and so on.

When working at plateau, what diesel engine faces is not only deteriorating combustion condition in cylinder but also severe deterioration of cooling radiator capacity of dynamic system [21]. Deterioration of in-cylinder combustion and cooling capacity make some high-temperature parts in cylinder like piston, cylinder cover and cylinder gasket accumulate excessive heat, which will lead these parts subjected to fatigue damage and failure [22]. However, there is a paucity of computation focusing on in-cylinder heat accumulation and dissipation among studies on diesel engine working in plateau environment [23]. In addition, several existed researches are limited to the area of combustion and emission [24]. In-cylinder heat dissipation affects thermal state of high-temperature parts and has further great effects on parts' stress condition and whole machine's reliability [25]. Therefore, it is necessary to research the performance and in-cylinder heat accumulation and dissipation of diesel engine working at plateau. There are some other researchers studying diesel engine working at plateau, the main focus of these articles are combustion and emission characteristics [26], effects of altitudes [27], two-stage turbocharging system [28], and altitude adaptability of turbocharging [29].

To provide a solution to aforesaid questions, this paper, based on orthogonal experiment design, radial basis function neural network and genetic algorithm, calculates and analyzes the optimal working state parameters of diesel engine at high altitude by focusing on three performance indexes such as power, torque, and in-cylinder heat dissipation. This approach is capable to determine the optimal working state parameters of diesel engine working at plateau in an efficient and accurate way, so as to maximize the overall engine's performance and bring down the thermal load of high-temperature parts. The work in this paper is mainly composed of the following parts. In the first place, a simulation model of diesel engine is established for computing and analyzing the effect of five working state parameters of diesel engine on its performance indexes in combination with orthogonal experiment. According to the results, four parameters are selected for subsequent calculation and analysis. Then, radial basis function neural network and calculation-derived data are used to exert learning and training on correspondences between four parameters and five indexes, and the results are verified using part of calculation-derived data. Through radial basis function neural network, discrete input parameters and output indexes are converted to continuous values to facilitate subsequent calculation and analysis. Next, genetic algorithm is employed together with radial basis function neural network to calculate the optimal working state parameters of diesel engine at 3700 m altitude and 2000 rpm. At last, the data from the bench test verify the accuracy of calculation outcome and the effectiveness of algorithms.

2. Establishment and Verification of Diesel Engine Simulation Model

2.1. Model Establishment

In this paper, certain heavy-duty diesel engine is selected as the research subject. Its structural parameters and performance indexes at plain condition are listed in Table 1. The simulation model of the diesel engine's left part is established with the software of GT-POWER, as shown in Figure 1. The main components of the model include the inlet and exhaust pipes, compressor, inlet and outlet value, oil injector, cylinders and turbine. The heat transfer model in cylinder is set as Woschni model, combustion model is set as turbulent flame model, and the oil injection model is set as InjAF-Ratio-Conn injection model. In the simulation model, we simplified the inlet and outlet pipes into rough cylindrical pipes.

Table 1. Structural parameters and performance indexes of diesel engine.

Parameters	Values
Structure	Turbocharging, four stroke
Cylinders	12 cylinders, V-type
Cylinder diameter/length of stroke (mm)	150/180

Table 1. *Cont.*

Parameters	Values
Compression ratio/total displacement (L)	13.5:1/38.8
Length of connecting rod (mm)	320
Rated power (kW)	537
Rated speed (rpm)	2000
Maximum torque (N·m)	2991
Speed at maximum torque (rpm)	1400

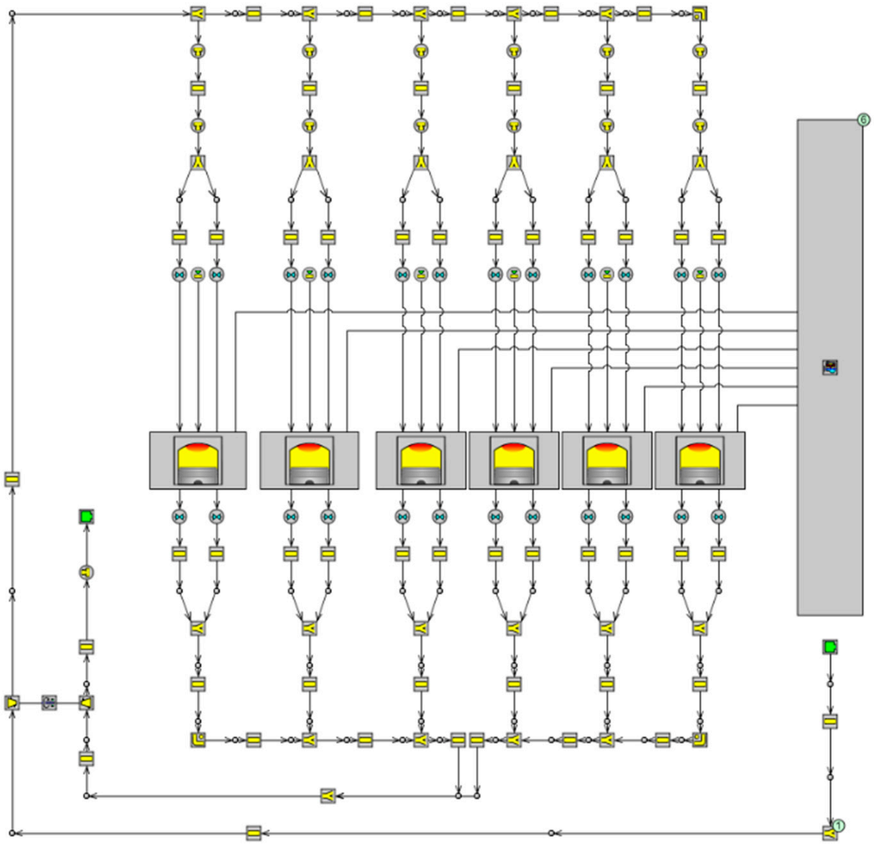

Figure 1. Simulation model of diesel engine.

Simulation model of the diesel engine is employed to figure out such performance indexes of diesel engine as its power, torque, in-cylinder heat dissipation, in-cylinder maximum pressure, highest exhaust temperature, and specific fuel consumption.

2.2. Test Equipment

This paper made use of the plateau-simulated diesel engine bench test lab to finish verification of the simulation model. Figure 2 is a schematic diagram of the bench test. The test system is mainly made up of control system, diesel engine and start moto, dynamo meter, combustion analysis system, and control unit. The control system can control the whole diesel engine bench test lab, measure and process the data. Diesel engine and start moto is the object of study and the core part of the bench. Dynamo meter can be used to measure the torque and power of the engine and calculate the in-cylinder heat dissipation. Combustion analysis system can adjust the inlet value, exhaust value and the oil atomizer of the engine to control the working state parameters. In the analysis system, P_1, P_2, P_3 are the control unit to adjust the oil atomizer, exhaust value and inlet value. P_2 can measure the highest exhaust temperature. The value of in-cylinder maximum pressure is measured by this analysis system too. The function of control unit is to create the plateau environment in the lab. The control unit is mainly made up of filter, cooling part, compressor, temperature control part, humidity control part and outlet cooling part. Figure 3 is the detail schematic diagram of the control unit. The test lab can simulate conditions at altitude ranging from 0–4500 m (with corresponding atmospheric pressure ranging from 101.3 kPa to 57.57 kPa) and apply accurate control and continuous regulation to inlet pressure, temperature, and humidity. The measuring and controlling accuracy of each device is listed in Table 2.

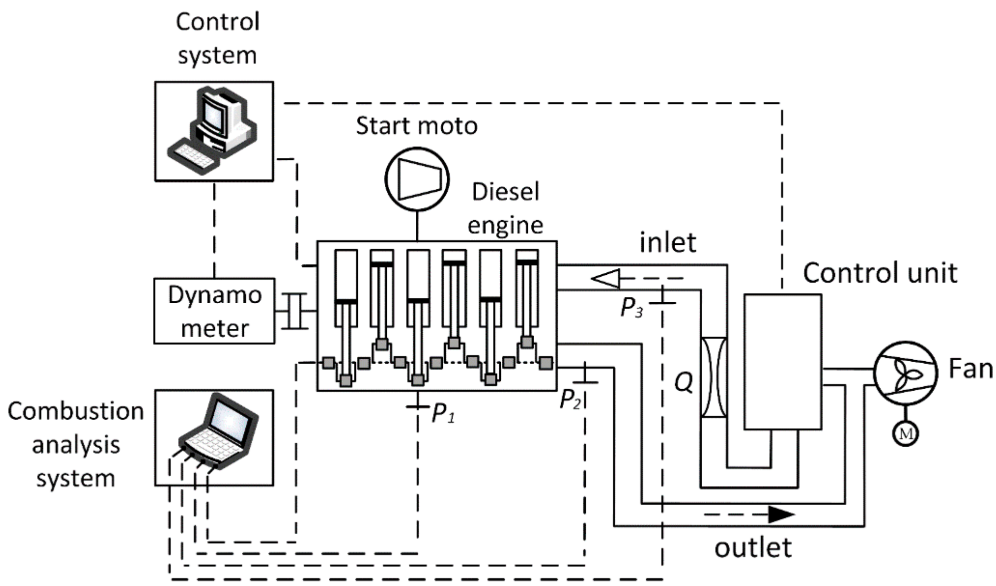

Figure 2. Schematic diagram of bench test.

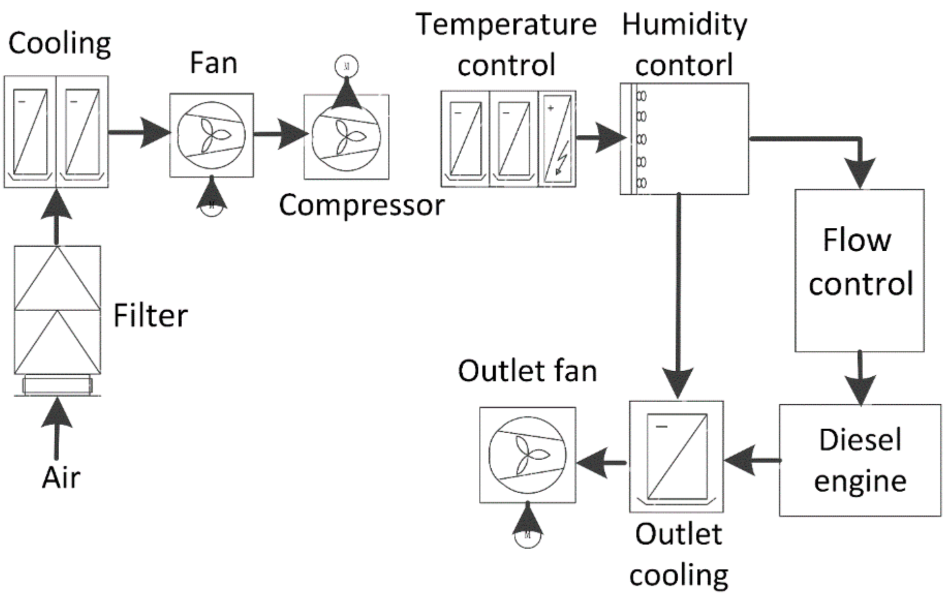

Figure 3. Schematic diagram of control unit.

Table 2. The accuracy and specification of each device.

Device	Specification	Accuracy
Dynamo meter	QZTI-QZ1030	Minus 0.1 Kw Minus 0.01 Nm
Combustion analysis system	LUBO-BO3010	Minus 0.1 K Minus 0.1 Pa

Table 2. *Cont.*

Device	Specification	Accuracy
P_1	BOSCH-HDEV-1 0445 110 317	Minus 1 mg
P_2	Aepes 15035	Minus 0.1 K
P_3	Aepes 15035	Minus 0.1 K
Cooling unit	ZHIXING-YWZX-18	Minus 1 K
Temperature unit	REYOU-RY01	Minus 0.1 K
Humidity unit	KZP-5-CA	Minus 0.1%

2.3. Model Verification

To verify the accuracy of the simulation model, we compare the data from the bench test lab and the simulation model. In Table 3, experimental values and calculated ones are compared and the errors are listed. According to the table, all the errors are minus 6%, proving the model's accuracy and its applicability to subsequent calculation and analysis.

Table 3. The comparison of calculated values with experimental ones.

Altitude/m	Speed/rpm	Power/kW			Torque/N * m			Specific Fuel Consumption/g/(kW * h)		
		Experiment	Calculation	Error/%	Experiment	Calculation	Error/%	Experiment	Calculation	Error/%
0	1400	463	475.8	2.82	3255	3245.3	0.32	222	220.2	0.91
	1600	525	518.6	−1.24	3205	3095.1	3.44	217	214.2	3.22
	1800	570	558.5	−2.15	3152	2969.8	5.81	221	219.6	3.87
	2000	588	594.7	1.11	2816	2839.4	−0.82	232	230.9	0.45
3700	1400	329	313.2	−4.93	2308	2186.3	5.31	261	252.7	3.10
	1600	377	384.9	2.01	2256	2297.1	−1.80	254	251.9	0.82
	1800	435	445.2	2.34	2317	2361.8	1.93	252	248.9	1.15
	2000	488	473.9	2.89	2335	2262.6	3.13	261	272.3	4.27

3. Orthogonal Experiment

3.1. Orthogonal Experiment Design

Orthogonal experiment is used hereby for calculation purpose to unveil the influence rules about how different working state parameters affect diesel engine's performance indexes. By referring to related literature [30], five parameters are finally selected as working state optimization parameters of diesel engine, including inlet valve opening angle α_{in}, exhaust valve opening angle α_{out}, supply quantity of diesel β_{oil}, advance angle of injection α_{oil}, and compressor flow coefficient β_{comp}. Each factor sets five levels to calculate and analyze, and thus $L_{25}(5^6)$ orthogonal experimental form is chosen for experimental design. In the form, there are all together six factors that contain five levels each, and it amounts to 25 sub-experiments. Values corresponding to five levels of each factor are listed in Table 4. In the table, the value of each level corresponding the relative change from the original value. For example, the level 1 of α_{in} is −0.1, which means that inlet valve opening angle of level 1 is 0.1 °C former than the original one. The level 2 of β_{oil} 185, which means in this level, the supply quantity of diesel is 185 mg every cycle in a single cylinder (the original value is 186 mg). Each level is one operating regime of the engine. During calculation, ambient conditions are set as 3700 m altitude and engine's speed is 2000 rpm. Evaluation indexes output by the orthogonal experiment include power P, torque N, in-cylinder heat dissipation Q, in-cylinder maximum pressure P_{mic}, and highest exhaust temperature T_{mo}.

Table 4. Values of five levels corresponding to five factors.

Parameters	Level1	Level2	Level3	Level4	Level5
α_{in}	−0.1	−0.05	0.00	0.05	0.1
α_{out}	−0.1	−0.05	0.00	0.05	0.1
β_{oil}	184	185	186	187	188
α_{oil}	−19.8	−19.9	−20.0	−20.1	−20.2
β_{comp}	0.98	0.99	1.00	1.01	1.02

3.2. Analysis of Results

Calculation is performed in above-mentioned 25 groups of experiments with established diesel engine working simulation model. The values of working state parameters and results of corresponding performance indexes are illustrated in Table 5.

Table 5. Values and results of the orthogonal experiment.

Number	α_{in}	α_{out}	β_{oil}	α_{oil}	β_{comp}	P kW	N Nm	Q kW	P_{mic} bar	T_{mo} K
1	−0.10	−0.10	184	−19.8	0.98	539.102	2573.942	442.446	84.020	628.571
2	−0.10	−0.05	185	−19.9	0.99	507.822	2424.594	477.706	74.135	677.565
3	−0.10	0.00	186	−20.0	1.00	505.106	2411.628	475.270	86.090	641.877
4	−0.10	0.05	187	−20.1	1.01	515.756	2462.477	454.106	74.063	649.079
5	−0.10	0.10	188	−20.2	1.02	518.199	2474.143	461.823	79.071	596.965
6	−0.05	−0.10	185	−20.0	1.01	417.989	1995.689	470.706	78.304	588.217
7	−0.05	−0.05	186	−20.1	1.02	435.060	2077.195	446.102	76.954	768.566
8	−0.05	0.00	187	−20.2	0.98	411.628	1965.316	448.109	73.542	591.593
9	−0.05	0.05	188	−19.8	0.99	499.071	2382.812	473.144	73.105	614.965
10	−0.05	0.10	184	−19.9	1.00	444.772	2123.565	466.648	92.540	656.302
11	0.00	−0.10	186	−20.2	0.99	433.272	2068.658	462.699	79.037	655.711
12	0.00	−0.05	187	−19.8	1.00	507.444	2422.792	440.439	82.539	659.692
13	0.00	0.00	188	−19.9	1.01	438.336	2092.835	447.014	83.898	618.242
14	0.00	0.05	184	−20.0	1.02	431.890	2062.058	446.278	88.036	652.239
15	0.00	0.10	185	−20.1	0.98	433.986	2072.067	454.402	86.292	697.843
16	0.05	−0.10	187	−19.9	1.02	433.639	2070.409	454.314	73.458	623.716
17	0.05	−0.05	188	−20.0	0.98	436.549	2084.302	444.473	82.248	676.876
18	0.05	0.00	184	−20.1	0.99	443.854	2119.18	465.871	95.166	670.871
19	0.05	0.05	185	−20.2	1.00	409.677	1956.001	474.346	72.792	643.354
20	0.05	0.10	186	−19.8	1.01	522.206	2493.273	454.277	84.033	626.009
21	0.10	−0.10	188	−20.1	1.00	425.114	2029.706	457.115	81.119	671.388
22	0.10	−0.05	184	−20.2	1.01	410.100	1958.022	446.018	88.958	720.008
23	0.10	0.00	185	−19.8	1.02	516.548	2466.257	472.338	81.741	616.278
24	0.10	0.05	186	−19.9	0.98	447.409	2136.156	471.257	76.117	610.700
25	0.10	0.10	187	−20.0	0.99	417.703	1994.322	450.209	81.416	646.779

Calculation results of performance indexes in Table 5 are summarized and put into analysis as shown in Table 6. In the table, I–V represent the sum of corresponding values of level 1 to 5 of each factor, and R denotes the difference between maximum and minimum value of I–V in different levels. Since power and torque of diesel engine exists the following equation [31], torque is not analyzed in the table.

$$P = \frac{Nn}{9549}, \tag{1}$$

where P denotes the power, N denotes the torque, and n denotes the speed of the engine.

Table 6. Statistical analysis of calculation results.

Indexes	Level	α_{in}	α_{out}	β_{oil}	α_{oil}	β_{comp}
P/kW	I	2585.985	2249.115	2269.720	2584.370	2268.675
	II	2208.520	2296.975	2286.020	2271.980	2301.720
	III	2244.930	2315.470	2343.055	2209.235	2292.115
	IV	2245.925	2303.800	2286.170	2253.770	2304.385
	V	2216.875	2336.865	2317.270	2182.875	2335.335
	R	377.465	87.7500	73.335	401.495	66.660
Q/kW	I	2301.350	2257.280	2267.260	2252.645	2253.685
	II	2274.705	2244.740	2272.495	2306.940	2319.630
	III	2243.830	2278.600	2309.605	2256.935	2313.815
	IV	2293.280	2319.130	2247.175	2270.595	2242.120
	V	2266.935	2280.360	2283.570	2292.995	2250.855
	R	57.520	74.390	62.430	54.295	77.510
P_{mic}/bar	I	237.380	395.940	448.720	405.440	402.215
	II	394.445	404.835	393.265	400.150	402.860
	III	419.800	420.435	402.230	416.090	415.080
	IV	407.695	384.110	385.020	413.595	409.255
	V	409.350	423.350	399.440	393.400	399.260
	R	25.355	39.240	63.700	22.690	15.820
T_{mo}/K	I	3194.060	3167.600	3327.995	3175.515	3205.580
	II	3219.645	3502.705	3223.255	3186.525	3265.895
	III	3283.725	3138.865	3332.865	3205.990	3272.615
	IV	3270.830	3170.335	3170.860	3457.750	3231.555
	V	3265.150	3253.895	3178.435	3207.630	3257.765
	R	89.665	363.840	162.005	282.235	67.035

As illustrated in Table 6, four working state indexes, i.e., diesel engine power P, in-cylinder heat dissipation Q, in-cylinder maximum pressure P_{mic}, and highest exhaust temperature T_{mo} are most affected by advance angle of injection α_{oil}, compressor flow coefficient β_{comp}, supply quantity of diesel β_{oil} and exhaust valve opening angle α_{out} seperately. Table 7 presents significance test and variance analysis results of how five factors affecting four indexes. In the table, SS denotes sum of square, F denotes F value, Sig denotes significance, if there is a * sign there, it means that the parameter has the significance influence on the state index. According to the table, inlet valve opening angle α_{in} and advance angle of injection α_{oil} has prominent effects on diesel engine power, effect of supply quantity of diesel β_{oil} is more prominent on in-cylinder heat dissipation Q and in-cylinder maximum pressure P_{mic}, and exhaust valve opening angle α_{out} has a greater influence on highest exhaust temperature T_{mo}.

Table 7. Significance test and variance analysis of calculation results.

Parameters	P/kW			Q/kW			P_{mic}/bar			T_{mo}/K		
	SS	F	Sig	SS	F	Sig	SS	F	Sig	SS	F	Sig
α_{in}	20,604.380	2.355	*	162.232	0.253		82.420	0.458		1159.354	0.161	
α_{out}	842.061	0.096		535.729	0.836		218.156	1.211		17,861.380	2.486	*
β_{oil}	690.909	0.079		1880.226	2.934	*	496.850	2.759	*	4998.952	0.696	
α_{oil}	21,148.790	2.417	*	145.835	0.228		70.496	0.391		11,282.880	1.571	
β_{comp}	463.675	0.053		479.930	0.749		32.460	0.180		616.487	0.086	

Taken together, the analysis above, for four indexes (i.e., power P, in-cylinder heat dissipation Q, in-cylinder maximum pressure P_{mic} and highest exhaust temperature T_{mo}), inlet valve opening angle α_{in}, exhaust valve opening angle α_{out}, supply quantity of diesel β_{oil} and advance angle of injection α_{oil} produce a significant effect on them. By contrast, compressor flow coefficient β_{comp} can affect in-cylinder heat dissipation Q only, but such an effect does not vary much from exhaust valve opening angle α_{out}. Moreover, variance analysis suggests this index to be insignificant for in-cylinder heat dissipation Q Therefore, in subsequent analysis, this article will ignore the effect of compressor flow coefficient β_{comp}, only inlet valve opening angle α_{in}, exhaust valve opening angle α_{out}, supply quantity of diesel β_{oil} and advance angle of injection α_{oil} are considered. Based on results provided in Tables 5 and 6, compressor flow coefficient β_{comp} is set to be 1.01 in following calculation. The results calculated from orthogonal experiment are discrete points, which cannot be directly applied to the following optimization. So, a kind of RBF-NN-based performance indexes prediction method is suggested on the basis of orthogonal experiment calculation results.

4. RBFNN-Based Performance Prediction Method

Radial basis function neural network (RBF-NN) is proposed to deal with the problem that four working state parameters and corresponding five performance indexes of the diesel engine are discrete points.

4.1. Fundamental Model

RBF-NN usually contains three single hidden layers, namely input layer composed of data or signal source, hidden layer of neuron kernel function, and output layer of linear weighting of neuron.

Corresponding mathematical model [5] is as follows:

$$y_i = \sum_{i=1}^{n_c} w_i g(\|x - c_i\| / \sigma_i) + b, \tag{2}$$

where x indicates input vector (the value of x are 4 to-be-optimized parameters of diesel engine: inlet valve opening angle α_{in}, exhaust valve opening angle α_{out}, supply quantity of diesel β_{oil} and advance angle of injection α_{oil}), w_i indicates output layer weight, $g(\|x - c_i\|/\sigma_i)$ indicates radial basis function, c_i indicates center of radial basis function, σ_i indicates width, b indicates output layer threshold value, n_c indicates number of neurons in hidden layer, $\|x - c_i\|$ indicates vector norm of distance from x to c_i.

Gaussian function is selected as radial basis function, so neuron i can be output as:

$$R_i(x) = exp\left(-\|x - c_i\|^2 / \left(2\sigma_i^2\right)\right), \tag{3}$$

Corresponding mapping relation is:

$$\mathrm{y} = f(x) = WR = \sum_{i=1}^{n_c} w_i R_i(x), \tag{4}$$

where W means weight of output layer, R means output value of neuron in hidden layer. What the model outputs are five performance indexes of diesel engine, namely power P, torque N, in-cylinder heat dissipation Q, in-cylinder maximum pressure P_{mic}, and highest exhaust temperature T_{mo}. In this article, the number of neurons in input layer is four, which corresponds to the four working state parameters. The number of neurons in output layer is five, which corresponds to the five performance indexes. The number of neurons in hidden layer is eight. The activation function in hidden layer is gaussian function. The activation function in output layer is tanh() function.

$$\tanh(x) = \frac{e^x - e^{-x}}{e^x + e^{-x}} \tag{5}$$

This article employed the orthogonal least square method to calculate the central parameters of neurons. Figure 4 is the schematic diagram of RBF-NN.

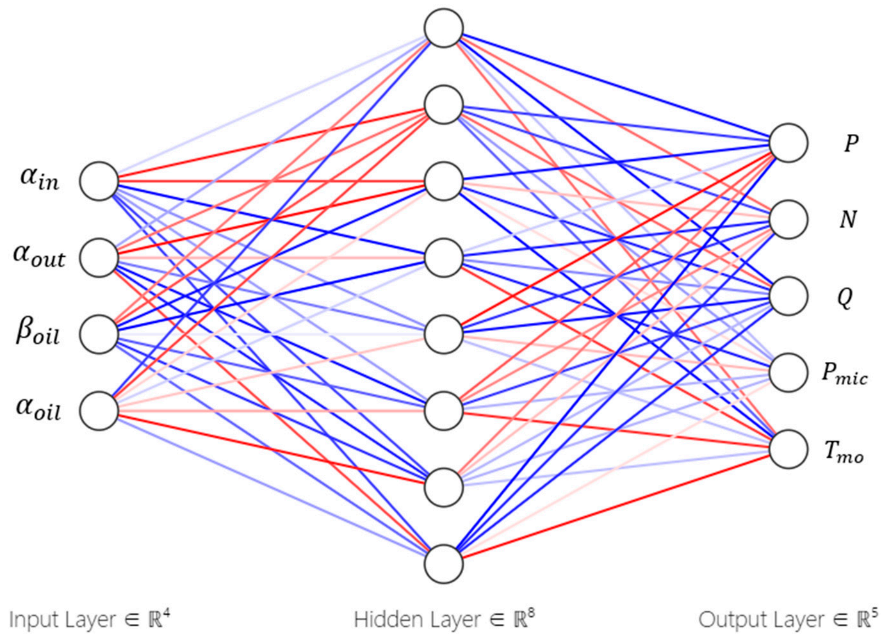

Figure 4. The schematic diagram of RBF-NN.

4.2. Training Samples

The established working simulation model is used in calculating all performance indexes of diesel engine working at 3700 m altitude and 2000 rpm. For four to-be-optimized parameters as input, progressive step is determined as one tenth of orthogonal experiment and five performance indexes are the corresponding output. Define every nine data as a sample, which include four to-be-optimized parameters and five corresponding performance indexes. Altogether, 241 samples of data are drawn from calculation, from which 221 are randomly selected as training samples, while the rest 20 as verification samples. The whole data are listed in the Table A1 in Appendix A.

The normalization of the data before analysis is applied using the following equation:

$$x_l = \frac{|x - x_{min}|}{x_{max} - x_{min}}, \tag{6}$$

where x_l denotes normalized value, x denotes original value, x_{max} denotes the maximum value under same factor, and x_{min} denotes the minimum value under same factor.

4.3. Training Results and Verification

RBF-NN is trained with 221 sets of normalized data and then verified with the rest 20 sets. The number of epochs is set as 200. The fitness value of the algorithm is 0.001. Part of results are demonstrated in Table 8. A comparison of original values with predicted ones is made in Figure 5. As revealed in Table 8 and Figure 5, RBF-NN can control errors concerning all performance indexes of diesel engine minus 4.6%, which testifies its accuracy and applicability to subsequent calculation and analysis. The MRE (Mean Relative Error), MSE (Mean Square Error) and RMSE (Root Mean Square Error) of the data listed in Table 9 also verify the accuracy of the prediction. Besides, this article conducted an experiment to test the accuracy of the RBFNN method, and the results are shown in the 6th paper section.

With RBF-NN, it is possible to extend the working state parameters limited to a few points to a continuous operation condition so that further calculation and analysis with GA and multi-objective optimization can proceed. Considering such reasons as computer configuration and the efficiency of training, progressive step of the training samples in this paper accounts for one tenth of data interval in orthogonal experiment and it can be adjusted flexibly when it necessary.

Table 8. The comparison of some original values with predicted ones in RBF-NN.

Number		**1**	**2**	**3**	**4**	**5**	**6**	**7**
α_{in}		−0.10	−0.10	−0.10	−0.07	−0.05	−0.05	−0.05
α_{out}		−0.05	0.00	0.07	−0.04	−0.06	0.01	0.07
β_{oil}		185.1	186.0	187.4	185.9	185.9	187.1	186.8
α_{oil}		−19.91	−20.00	−20.14	−20.06	−20.09	−20.16	−19.83
P/kW	Original	501.593	505.106	514.918	455.007	437.493	414.409	492.336
	Prediction	483.101	482.585	522.203	470.095	434.941	432.271	490.022
	Error	3.69%	4.46%	−1.41%	−3.32%	0.58%	−4.31%	0.47%
N/Nm	Original	2394.856	2411.628	2458.475	2172.431	2088.808	1978.597	2350.660
	Prediction	2357.363	2444.548	2441.914	2123.126	2010.279	2055.681	2341.463
	Error	1.57%	−1.37%	0.67%	2.27%	3.76%	−3.90%	0.39%
Q/kW	Original	471.859	475.270	455.586	475.307	452.847	444.221	480.521
	Prediction	462.525	486.206	474.749	496.970	448.007	425.008	482.631
	Error	1.98%	−2.30%	−4.21%	−4.56%	1.07%	4.32%	−0.44%
P_{mic}/bar	Original	74.446	86.090	75.799	79.753	77.826	72.455	80.498
	Prediction	72.683	85.040	75.829	78.956	77.088	74.190	81.949
	Error	2.37%	1.22%	−0.04%	1.00%	0.95%	−2.39%	−1.80%
T_{mo}/K	Original	666.086	641.877	626.026	600.012	757.700	585.506	639.783
	Prediction	645.877	664.541	633.775	586.622	764.748	599.070	643.169
	Error	3.03%	−3.53%	−1.24%	2.23%	−0.93%	−2.32%	−0.53%

Table 9. The MRE, MSE, RMSE of the data.

Parameter	***P*/kW**	***N*/Nm**	***Q*/kW**	**P_{mic}/bar**	**T_{mo}/K**
MRE	−0.0017	0.0061	0.0067	0.0067	0.0052
MSE	0.0212	0.0080	0.0557	0.0103	0.0124
RMSE	0.1456	0.0895	0.2360	0.1017	0.1114

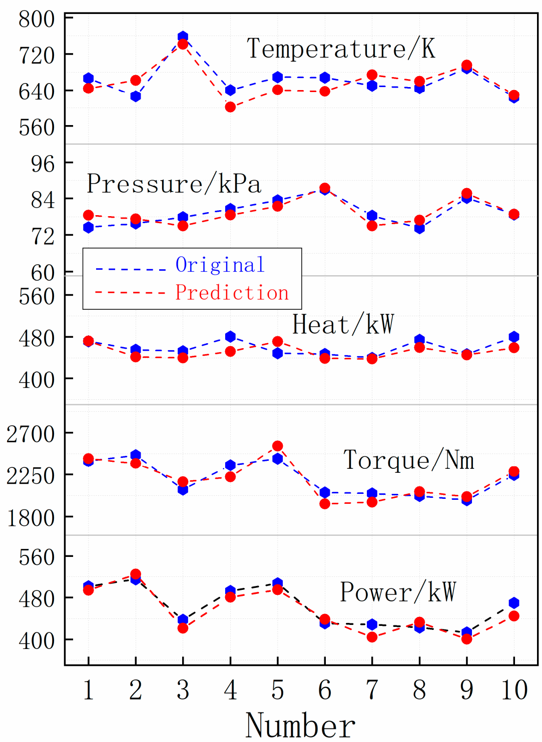

Figure 5. The comparison of original values with calculated ones in RBF-NN.

5. RBF-NN and GACMOO Based Multi-Objective Optimization of State Parameters

On the basis of analysis above, genetic algorithm-based cycle multi-objective optimization method (GACMOO) is proposed. When combined with RBF-NN algorithm described above, it can simultaneously solve a string of problems such as wide scope of initial optimization parameters, non-intelligent decision-making process, and difficulty in taking into account several optimization objects at one time [32].

5.1. Operating Process

In this paper, RBF-NN and GA are adopted to perform a cycle multi-objective optimization on three performance indexes: diesel engine power P, torque N and in-cylinder heat dissipation Q. This algorithm is called Radial Basis Function Neural Network & Genetic Algorithm Cycle Multi-Objective Optimization (RBFNN & GACMOO).

The basic procedure of using RBFNN & GACMOO algorithm to perform multi-objective optimization on diesel engine operating process is as follows:

- (1) Make prediction about diesel engine's performance with RBF-NN:

Initial values of 4 to-be-optimized parameters (α_{in}, α_{out}, β_{oil}, and α_{oil}) are introduced into trained RBF-NN to predict 5 performance parameters (P, N, Q, P_{mic}, and T_{mo}).

- (2) Calculate functional value of fitness:

Fitness function values of three performance indexes are figured out by combining boundary conditions formula with fitness function;

- (3) Determine optimal performance indexes of diesel engine:

GA is employed to calculate optimal values of performance functions. After getting the results of each cycle, the latest optimal values derived from calculation are compared with existing optimal values. If the former turns out to be better, it will be saved; otherwise, optimization parameters will be updated for continuous calculation and next cycle.

- (4) Update weight coefficients of fitness function:

The GA-derived optimal values of diesel engine's four to-be-optimized parameters and corresponding optimal performance indexes are used to substitute data in column five of Table 10. Then data in the table are re-arranged by a descending order and then used to calculate weight coefficients of fitness function again;

- • (5) Iterative computations:

Step 1 through 4 are repeated until weight coefficients no longer changes.

Specific operating process is as demonstrated in Figure 6.

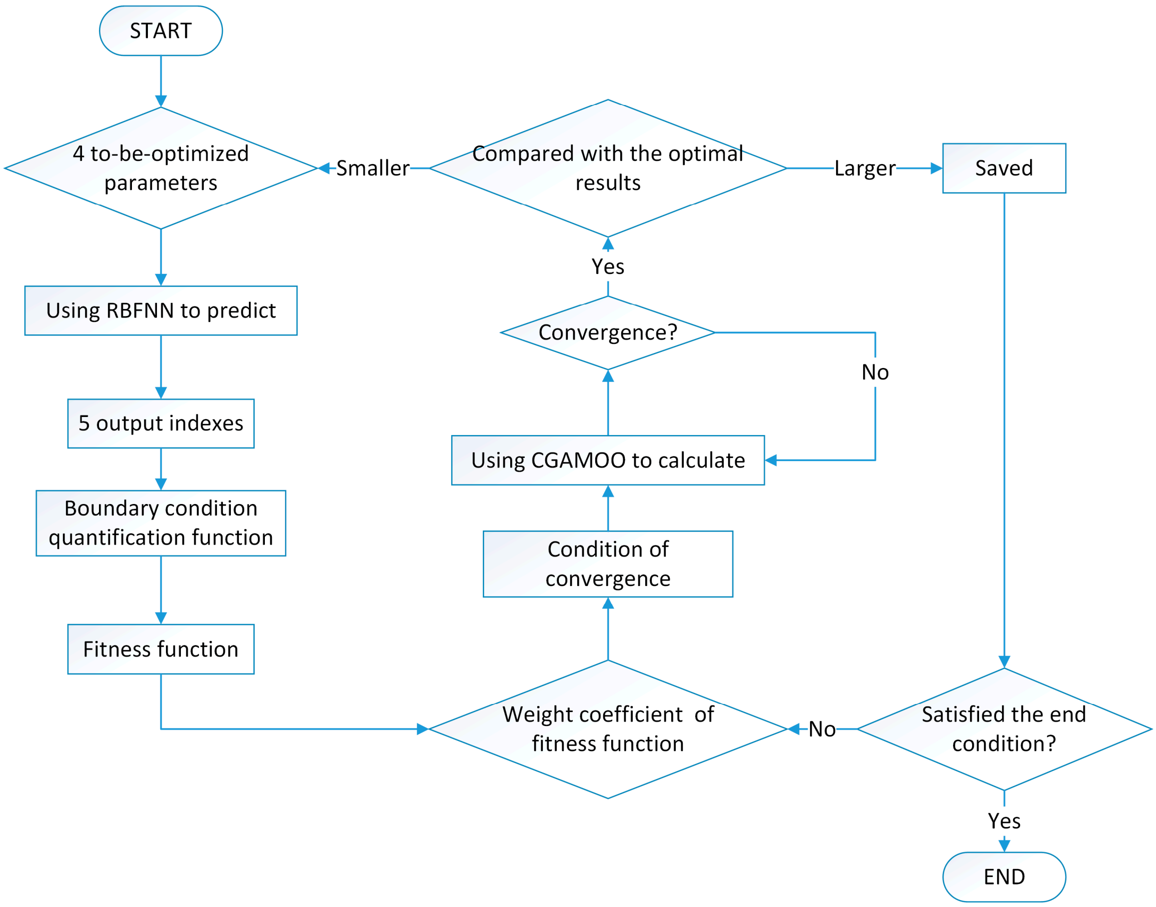

Figure 6. Operating process chart of RBFNN & GACMOO method.

5.2. Boundary Condition Quantification Function

According to the practical experience and the results in Tables 3 and 5, when diesel engine works at 3700 m altitude and 2000 rpm, its power P, torque N, in-cylinder heat dissipation Q and in-cylinder maximum pressure P_{mic} cannot be lower than 470 kW, 2330 Nm, 450 kW, and 70 bar, respectively, while highest exhaust temperature T_{mo} cannot exceed 700 K. In order to embody limitations on those indicators in the algorithm, following boundary condition quantification functions are introduced for those related indicators:

$$Q_1(X) = Q_p(X) = P(X)/470 - 1, \tag{7}$$

$$Q_2(X) = Q_n(X) = N(X)/2330 - 1, \tag{8}$$

$$Q_3(X) = Q_q(X) = Q(X)/450 - 1, \tag{9}$$

$$Q_4(X) = Q_{mic}(X) = P_{mic}(X)/70 - 1, \tag{10}$$

$$Q_5(X) = Q_{mo}(X) = 1 - T_{mo}(X)/700, \tag{11}$$

$$(X) = (\alpha_{in}, \alpha_{out}, \beta_{oil}, \alpha_{oil})^T, \tag{12}$$

where $Q_p(X)$, $Q_n(X)$, $Q_q(X)$, $Q_{mic}(X)$, and $Q_{mo}(X)$ indicate working condition quantification function of diesel engine's power, torque, in-cylinder heat dissipation, in-cylinder maximum pressure and highest exhaust temperature, respectively; while $P(X)$, $N(X)$, $Q(X)$, $P_{mic}(X)$, and $T_{mo}(X)$ represent diesel engine's power, torque, in-cylinder heat dissipation, in-cylinder maximum pressure and highest exhaust temperature when the input parameter is X, respectively.

5.3. Fitness Function

The optimization process of the GA is called "natural selection law", which looks for and selects optimal objectives through fitness function. Fitness function, on the other hand, should be designed on the basis of specific model-influencing factors, as its quality directly decides the algorithm's calculating accuracy and efficiency [33].

The main goal of this paper is to figure out the optimal performance indexes of diesel engine in plateau environment by adjusting its working state parameters. As to diesel engine, primary performance indexes to be considered include its power, torque, in-cylinder heat dissipation, in-cylinder maximum pressure and highest exhaust temperature. Therefore, the fitness function must be related with these indexes. In fact, the in-cylinder pressure directly correlates with the power and torque, and the exhaust temperature partly correlates with the in-cylinder heat dissipation. To reduce the cost of calculation, we ignore the effect of in-cylinder maximum pressure and highest exhaust temperature when determining the fitness function.

Thus, three objective-optimizing fitness functions are introduced hereby:

$$P_{goal} = P(X) - \sum_{i=1}^{5} \alpha_i Q_i(X), \tag{13}$$

$$T_{goal} = N(X) - \sum_{j=1}^{5} \beta_j Q_j(X), \tag{14}$$

$$Q_{goal} = Q(X) - \sum_{l=1}^{5} \gamma_l Q_l(X), \tag{15}$$

where, P_{goal}, T_{goal}, and Q_{goal} represent objective-optimizing functions for diesel engine's power, torque and in-cylinder heat dissipation, respectively, α_i, β_j, and γ_l are weight coefficients corresponding to quantification functions in the objective-optimizing fitness functions.

5.4. Initial Value of Weight Coefficients

Through the analysis of diesel engine working process, boundary condition quantification function and fitness function for plateau state optimization are set up. In addition, the core bridge between those two functions is weight coefficients [34], which will be determined with the following procedure.

Since every fitness function contains five unknown weight coefficients, five sets of data are required for obtaining a solution. The first five relatively optimal solutions concerning power, torque and heat dissipation in Table 5 calculating from orthogonal experiments are substituted into the formula above, and fitness function value is set to be 0, then following formulas can be derived:

$$P(X_{i-k}) - \sum_{i=1}^{5} \alpha_i Q_i(X_{i-k}) = 0, \tag{16}$$

$$N\left(X_{j-k}\right) - \sum_{j=1}^{5} \beta_j Q_j\left(X_{j-k}\right) = 0, \tag{17}$$

$$Q(X_{l-k}) - \sum_{l=1}^{5} \gamma_l Q_l(X_{l-k}) = 0, \tag{18}$$

where value of k ranges from 1 to 5, X_{i-k}, X_{j-k}, and X_{l-k} corresponds to the first five optimal values of calculated power, torque and heat dissipation. Specific values and computed indexes are listed in Table 10.

Table 10. Values and corresponding results of X.

Group 1: Optimal $P(X_{i-k})$	X_{i-1}	X_{i-2}	X_{i-3}	X_{i-4}	X_{i-5}
α_{in}	−0.10	−0.10	0.05	−0.05	0.10
α_{out}	−0.05	0.00	0.05	0.05	0.00
β_{oil}	185	186	185	188	185
α_{oil}	−19.9	−20.0	−20.2	−19.8	−19.8
$P(X_{i-k})$/kW	507.820	505.100	409.670	499.070	516.540
$N(X_{i-k})$/Nm	2424.590	2411.620	1956.000	2382.810	2466.250
$Q(X_{i-k})$/kW	477.700	475.260	474.340	473.140	472.330
$P_{mic}(X_{i-k})$/bar	74.130	86.080	72.792	73.100	81.740
$T_{mo}(X_{i-k})$/K	677.560	641.870	643.350	614.960	616.270
Group 2: Optimal $N(X_{j-k})$	X_{j-1}	X_{j-2}	X_{j-3}	X_{j-4}	X_{j-5}
α_{in}	−0.10	0.05	−0.10	0.10	−0.10
α_{out}	−0.10	0.10	0.10	0.00	0.05
β_{oil}	184	186	188	185	187
α_{oil}	−19.8	−19.8	−20.2	−19.8	−20.1
$P(X_{j-k})$/kW	539.100	522.210	518.200	516.550	0515.760
$N(X_{j-k})$/Nm	2573.940	2493.270	2474.140	2466.260	2462.480
$Q(X_{j-k})$/kW	442.450	454.280	461.820	472.340	454.110
$P_{mic}(X_{j-k})$/bar	84.020	84.030	79.070	81.740	74.060
$T_{mo}(X_{j-k})$/K	628.570	626.010	596.960	616.280	649.080
Group 3: Optimal $Q(X_{l-k})$	X_{l-1}	X_{l-2}	X_{l-3}	X_{l-4}	X_{l-5}
α_{in}	−0.10	−0.10	0.05	−0.05	0.10
α_{out}	−0.05	0.00	0.05	0.05	0.00
β_{oil}	185	186	185	188	185
α_{oil}	−19.9	−20.0	−20.2	−19.8	−19.8
$P(X_{l-k})$/kW	507.820	505.110	409.680	499.070	516.550
$N(X_{l-k})$/Nm	2424.590	2411.630	1956.000	2382.810	2466.260
$Q(X_{l-k})$/kW	477.710	475.270	474.350	473.140	472.340
$P_{mic}(X_{l-k})$/bar	74.140	86.090	72.790	73.110	81.740
$T_{mo}(X_{l-k})$/K	677.570	641.880	643.350	614.970	616.280

Through calculation, values of 15 weight coefficients are determined and shown in Table 11.

Table 11. Calculation-derived values of weight coefficients.

Coefficients	Values	Coefficients	Values	Coefficients	Values
α_1	−2846.80	β_1	−3486.42	γ_1	−3516.43
α_2	−6782.73	β_2	−8214.83	γ_2	−7814.67
α_3	2438.72	β_3	2982.07	γ_3	2461.81
α_4	4046.54	β_4	4243.16	γ_4	4123.19
α_5	3229.59	β_5	2858.96	γ_5	3978.96

5.5. Updating of Weight Coefficients

Weight coefficients derived from calculation above are substituted into fitness functions of three to-be-optimized objectives as initial values for determining the optimal working state parameters and performance indexes of diesel engine. Afterwards, weight coefficients are re-computed on the basis of the calculation outcome. Detailed process is listed below:

- (1) Substitute weight coefficients into fitness functions of three to-be-optimized objectives for calculation;

- (2) Substitute X_{i-5}, X_{j-5} and X_{l-5} in Table 10 with newest results of diesel engine's four to-be-optimized parameters and five corresponding optimal performance indexes;
- (3) Re-arrange data in five columns of group 1, 2 and 3 in Table 10 in a descending order with as $P(X_{i-k})$, $N\left(X_{j-k}\right)$ and $Q(X_{l-k})$ measuring criteria;
- (4) Set value of fitness function to be 0, and combine it with data in updated Table 10 for calculation of weight coefficients again;
- (5) Repeat step (1) to (4) as per iterative calculation process in Figure 6 until the data satisfies the convergence condition.

5.6. Condition of Convergence

During calculation, following condition of convergence is established:

$$C_1 = \left(\left|P'^{(n)}_{goal} - P'^{(n-1)}_{goal}\right|\right)/P'^{(n)}_{goal} < 0.03, \tag{19}$$

$$C_2 = \left(\left|N'^{(n)}_{goal} - N'^{(n-1)}_{goal}\right|\right)/T'^{(n)}_{goal} < 0.03, \tag{20}$$

$$C_3 = \left(\left|Q'^{(n)}_{goal} - Q'^{(n-1)}_{goal}\right|\right)/E'^{(n)}_{goal} < 0.03, \tag{21}$$

where, $P'^{(n)}_{goal}$, $P'^{(n-1)}_{goal}$, $N'^{(n)}_{goal}$, $N'^{(n-1)}_{goal}$, $Q'^{(n)}_{goal}$, and $Q'^{(n-1)}_{goal}$ represent fitness function values of diesel engine's power, torque and heat dissipation resulting from No. n and No. n-1 cycle computation.

Quadric sum of three convergence indexes is monitored during the calculation:

$$C_4 = C_1^2 + C_2^2 + C_3^2, \tag{22}$$

In calculation, iteration number is set to last 350 cycles. What Figure 7 presents is change rules of C value as iteration goes on after weight coefficients is no longer updated.

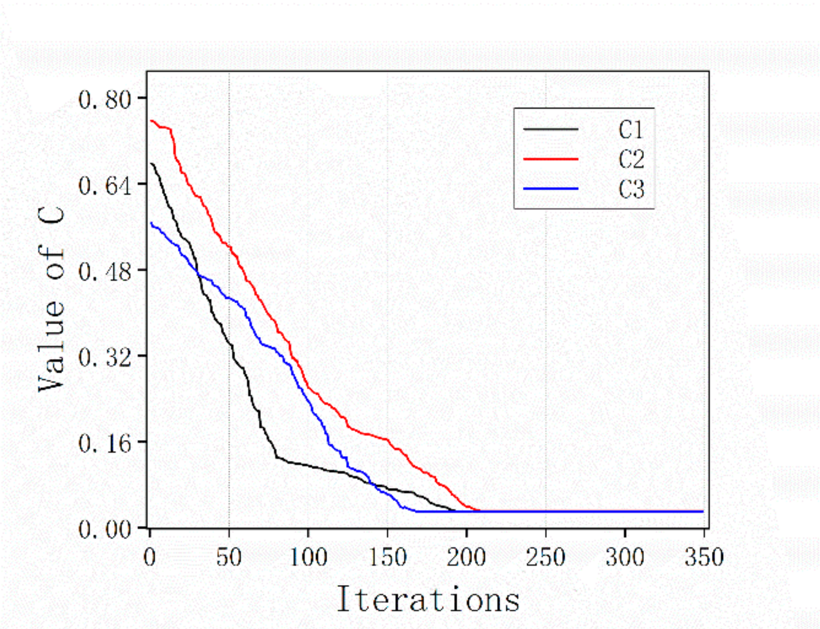

Figure 7. Change of C value.

5.7. Analysis of Calculation Results

Values of optimal torque, power, and heat dissipation of diesel engines are figured out as shown in Table 12. As revealed by results, when working in optimal state, the engine's power, torque, and in-cylinder heat dissipation are 2520.93 Nm, 528.45 kW, and 465.32 kW respectively.

Table 12. Calculation results of diesel engine's optimal state parameters.

Parameters	α_{in}	α_{out}	β_{oil}	α_{oil}	P/kW	N/Nm	Q/kW	P_{mic}/bar	T_{mo}/K
Values	−0.09	−0.09	184.4	−19.8	528.5	2520.930	465.320	80.510	648.180

6. Verification with Bench Test

To verify whether the RBF-NN & GACMOO method is both effective and accurate in diesel engine's optimization, an experiment test on diesel engine's performance in plateau environment was carried out.

Diesel engine was tested with aforesaid bench about its working state in plateau environment. Different test variables are set as shown in Table 13.

Table 13. The configuration of variables in verification experiment.

Number	α_{in}	α_{out}	β_{oil}	α_{oil}	β_{comp}
1	−0.09	−0.09	184.4	−19.8	1.01
2	−0.05	−0.07	185.6	−20.1	1.01
3	−0.05	0.07	186.4	−19.8	1.01
4	0.00	−0.04	187.2	−19.8	1.01
5	0.05	0.03	184.5	−20.2	1.01
6	0.10	−0.02	184.7	−19.9	1.01

In Table 13, the first group of experiment is the recommendation configurations of diesel engine parameters resulting from RBFNN & GACMOO, whereas the second to sixth use five sets of parameters randomly selected from Table A1 for RBF-NN training and verification. Due to limited experimental conditions, it is impossible to directly measure in-cylinder heat dissipation of diesel engine by now. Therefore, only power and torque got measured. Experimental values and predicted ones of diesel engine power and torque are compared as demonstrated in Tables 14 and 15.

Table 14. Comparison of experimental values with predicted ones of diesel engine power (kW).

Number	Experimental Value	Predicted Value	Error
1	525.20	528.45	−0.62%
2	447.94	435.92	2.68%
3	500.71	475.93	4.95%
4	519.48	501.64	3.43%
5	405.92	425.56	−4.84%
6	503.71	483.10	4.09%

Table 15. Comparison of experimental values and predicted ones of diesel engine torque (Nm).

Number	Experiment Value	Predicted Value	Error
1	2549.19	2520.93	1.11%
2	2137.06	2081.32	2.61%
3	2403.92	2272.32	5.47%
4	2490.89	2395.12	3.84%
5	1955.49	2031.86	−3.91%
6	2406.38	2306.60	4.15%

As shown in Tables 14 and 15, errors between experimental values and predicted ones are all minus engineering tolerance range i.e., 6%, which proves accuracy of results and effectiveness of RBFNN & GACMOO algorithm. It is worth pointing out that the error may partly from the measurement equipment of the experiment instead of totally from the trained RBF-NN.

7. Conclusions

The work completed in this paper mainly consists of:

(1) A simulation model is established for diesel engine working in plateau environment. Using the diesel engine bench test lab to verify the accuracy of the model.
(2) Using orthogonal experiment approach to calculate and analyze the rules that how five working state parameters (inlet valve opening angle, exhaust valve opening angle, supply quantity of diesel, advance angle of injection, and compressor flow coefficient) affecting its five performance indexes (power, torque, in-cylinder heat dissipation, in-cylinder maximum pressure, and highest exhaust temperature) of diesel engine. Results indicate inlet valve opening angle, exhaust valve opening angle, supply quantity of diesel and advance angle of injection are more prominent in affecting performance indexes, thus only those four parameters are considered in subsequent calculation and analysis.
(3) A prediction model is created to connect four working state parameters and five performance indexes of diesel engine on the basis of RBFNN method. The model is further trained with 221 samples which calculated from working simulation model, and predicting results are verified in term of its accuracy. Use of RBF-NN helps to serialize discrete working state parameters and corresponding performance indexes so as to facilitate the following calculation and optimization.
(4) Based on the above analysis, a multi-objective optimization approach called RBFNN & GACMOO method is proposed, which is used to find the optimal working state parameters of diesel engine at 3700 m altitude and 2000 rpm condition. In this method, the boundary condition quantification function, fitness function and its weight coefficients should be identified and quantified separately.
(5) Bench test verification indicates that optimal results conform to requirements of engineering accuracy. The solution can minimize in-cylinder heat dissipation and thermal load of high-temperature parts, while maintaining relatively insignificant reduction in power and torque of diesel engine working at plateau.

After establishing diesel engine simulation model and conducting an orthogonal experiment, this paper proposes a multi-objective optimization approach named RBFNN & GACMOO specific for working state of diesel engine at plateau on the basis of Radial Basis Function Neural Network and Genetic Algorithm Cycle Multi-Objective Optimization. The proposed approach can not only guarantee a reasonable power and torque for diesel engine working at plateau environment, but also minimize in-cylinder heat accumulation and subsequent lower thermal load on high-temperature parts, thus it is able to improve the service life and reliability of the whole engine. The model and algorithm can be applied to the calculation and analysis of diesel engine's optimal working state parameters at various altitudes and rpms and offer corresponding specific control strategies. The present research will be helpful to improve working performance and reliability of heavy-duty diesel engine working at plateau.

Author Contributions: Conceptualization, J.L. and Y.D.; methodology, Y.L. and Y.D.; validation, Y.D., Y.L., X.Q. and Y.J.; data curation, Q.K.; writing—original draft preparation, T.W.; Writing—Review and editing, X.Z. and J.L.; supervision, Y.D. funding acquisition, J.L.; writing—review& editing, S.Z. All authors have read and agreed to the published version of the manuscript.

Funding: This research received no external funding.

Conflicts of Interest: The authors declare no conflict of interest.

Appendix A

Table A1. Whole dataset for the RBF neural network analysis.

Number	α_{in}	α_{out}	β_{oil}	α_{oil}	P kW	N Nm	Q kW	P_{mic} bar	T_{mo} K
1	−0.100	−0.100	184.0	−19.80	539.102	2573.942	442.446	84.020	628.571
2	−0.100	−0.095	184.1	−19.81	536.270	2560.420	446.218	83.077	633.820
3	−0.100	−0.090	184.2	−19.82	540.706	2581.603	456.129	83.253	647.787
4	−0.100	−0.085	184.3	−19.83	531.821	2539.181	454.823	81.376	645.824
5	−0.100	−0.080	184.4	−19.84	526.289	2512.765	456.289	80.020	647.798
6	−0.100	−0.075	184.5	−19.85	530.274	2531.795	466.064	80.106	661.568
7	−0.100	−0.070	184.6	−19.86	529.003	2525.724	471.326	79.390	668.930
8	−0.100	−0.065	184.7	−19.87	525.665	2509.786	474.768	78.361	673.708
9	−0.100	−0.060	184.8	−19.88	512.997	2449.305	469.665	75.952	666.363
10	−0.100	−0.055	184.9	−19.89	501.231	2393.129	465.161	73.695	659.872
11	−0.100	−0.050	185.0	−19.90	507.822	2424.594	477.706	74.135	677.565
12 *	−0.100	−0.045	185.1	−19.91	501.593	2394.856	471.859	74.446	666.086
13	−0.100	−0.040	185.2	−19.92	514.717	2457.516	484.217	77.648	680.258
14	−0.100	−0.035	185.3	−19.93	510.485	2437.309	480.247	78.255	671.433
15	−0.100	−0.030	185.4	−19.94	510.314	2436.493	480.098	79.474	667.974
16	−0.100	−0.025	185.5	−19.95	511.622	2442.738	481.341	80.928	666.440
17	−0.100	−0.020	185.6	−19.96	513.131	2449.944	482.772	82.422	665.147
18	−0.100	−0.015	185.7	−19.97	506.703	2419.256	476.737	82.631	653.593
19	−0.100	−0.010	185.8	−19.98	515.106	2459.375	484.655	85.264	661.153
20	−0.100	−0.005	185.9	−19.99	512.027	2444.675	481.770	86.011	653.939
21 *	−0.100	0.000	186.0	−20.00	505.106	2411.628	475.270	86.090	641.877
22	−0.090	0.000	186.2	−19.99	507.442	2422.781	480.987	87.423	651.077
23	−0.080	0.000	186.4	−19.98	498.529	2380.227	476.091	86.832	645.931
24	−0.070	0.000	186.6	−19.97	486.357	2322.113	468.027	85.658	636.464
25	−0.060	0.000	186.8	−19.96	474.142	2263.790	459.840	84.455	626.796
26	−0.050	0.000	187.0	−19.95	471.203	2249.761	460.636	84.901	629.368
27	−0.040	0.000	187.2	−19.94	458.771	2190.400	452.134	83.631	619.228
28	−0.030	0.000	187.4	−19.93	459.529	2194.019	456.645	84.770	626.917
29	−0.020	0.000	187.6	−19.92	451.304	2154.751	452.279	84.264	622.437
30	−0.010	0.000	187.8	−19.91	446.959	2134.007	451.807	84.485	623.320
31	−0.100	0.050	187.0	−20.10	515.756	2462.477	454.106	74.063	649.079
32	−0.100	0.055	187.1	−20.11	520.874	2486.911	459.173	75.268	649.948
33	−0.100	0.060	187.2	−20.12	506.445	2418.023	447.000	73.640	626.533
34	−0.100	0.065	187.3	−20.13	516.084	2464.043	456.063	75.506	632.947
35 *	−0.100	0.070	187.4	−20.14	514.918	2458.475	455.586	75.799	626.026
36	−0.100	0.075	187.5	−20.15	514.574	2456.832	455.835	76.211	620.124
37	−0.100	0.080	187.6	−20.16	522.099	2492.761	463.062	77.794	623.635
38	−0.100	0.085	187.7	−20.17	521.798	2491.327	463.355	78.218	617.727
39	−0.100	0.090	187.8	−20.18	513.222	2450.378	456.289	77.393	602.121
40	−0.100	0.095	187.9	−20.19	508.442	2427.556	452.584	77.127	591.116
41	−0.100	0.100	188.0	−20.20	518.199	2474.143	461.823	79.071	596.965
42	−0.095	0.080	187.7	−20.18	504.367	2408.099	459.241	78.402	591.619
43	−0.090	0.060	187.4	−20.16	491.539	2346.854	457.441	77.869	587.307
44	−0.085	0.040	187.1	−20.14	489.885	2338.958	466.153	79.123	596.470
45	−0.080	0.020	186.8	−20.12	478.885	2286.438	466.126	78.891	594.421
46	−0.075	0.000	186.5	−20.10	475.640	2270.944	473.781	79.956	602.144
47	−0.070	−0.020	186.2	−20.08	457.149	2182.657	466.210	78.452	590.522
48 *	−0.065	−0.040	185.9	−20.06	455.007	2172.431	475.307	79.753	600.012
49	−0.060	−0.060	185.6	−20.04	433.346	2069.010	463.914	77.618	583.656
50	−0.055	−0.080	185.3	−20.02	421.109	2010.583	462.242	77.116	579.593
51	−0.050	−0.100	185.0	−20.00	417.989	1995.689	470.706	78.304	588.217
52	−0.050	−0.095	185.1	−20.01	420.116	2005.842	468.714	78.247	606.857
53	−0.050	−0.090	185.2	−20.02	417.701	1994.311	461.693	77.348	618.801
54	−0.050	−0.085	185.3	−20.03	415.550	1984.041	455.046	76.507	630.843
55	−0.050	−0.080	185.4	−20.04	432.640	2065.642	469.351	79.196	672.517
56	−0.050	−0.075	185.5	−20.05	419.552	2003.151	450.910	76.360	667.301
57	−0.050	−0.070	185.6	−20.06	435.926	2081.327	464.136	78.886	708.939

Table A1. *Cont.*

Number	α_{in}	α_{out}	β_{oil}	α_{oil}	P kW	N Nm	Q kW	P_{mic} bar	T_{mo} K
58	−0.050	−0.065	185.7	−20.07	429.338	2049.873	452.849	77.251	713.462
59	−0.050	−0.060	185.8	−20.08	427.195	2039.644	446.372	76.428	724.944
60 *	−0.050	−0.055	185.9	−20.09	437.493	2088.808	452.847	77.826	757.700
61	−0.050	−0.050	186.0	−20.10	435.060	2077.195	446.102	76.954	768.566
62	−0.050	−0.045	186.1	−20.11	428.268	2044.764	441.714	75.825	743.148
63	−0.050	−0.040	186.2	−20.12	425.214	2030.183	441.150	75.357	724.381
64	−0.050	−0.035	186.3	−20.13	432.407	2064.525	451.271	76.707	722.789
65	−0.050	−0.030	186.4	−20.14	425.435	2031.241	446.640	75.544	697.364
66	−0.050	−0.025	186.5	−20.15	423.072	2019.958	446.818	75.200	679.643
67	−0.050	−0.020	186.6	−20.16	428.779	2047.204	455.570	76.291	674.620
68	−0.050	−0.015	186.7	−20.17	421.022	2010.170	450.034	74.987	648.327
69	−0.050	−0.010	186.8	−20.18	418.245	1996.911	449.784	74.568	629.896
70	−0.050	−0.005	186.9	−20.19	406.757	1942.063	440.103	72.595	598.673
71	−0.050	0.000	187.0	−20.2	411.628	1965.316	448.109	73.542	591.593
72 *	−0.050	0.005	187.1	−20.16	414.409	1978.597	444.221	72.455	585.506
73	−0.050	0.010	187.2	−20.12	436.443	2083.798	460.853	74.708	606.449
74	−0.050	0.015	187.3	−20.08	432.215	2063.611	449.745	72.464	590.887
75	−0.050	0.020	187.4	−20.04	442.358	2112.039	453.767	72.669	595.228
76	−0.050	0.025	187.5	−20.00	452.735	2161.585	457.982	72.902	599.816
77	−0.050	0.030	187.6	−19.96	459.834	2195.479	458.880	72.607	600.058
78	−0.050	0.035	187.7	−19.92	468.496	2236.834	461.358	72.564	602.371
79	−0.050	0.040	187.8	−19.88	478.888	2286.451	465.518	72.783	606.877
80	−0.050	0.045	187.9	−19.84	485.888	2319.871	466.380	72.487	607.082
81	−0.050	0.050	188.0	−19.8	499.071	2382.812	473.144	73.105	614.965
82	−0.050	0.055	187.6	−19.81	494.763	2362.248	473.569	75.219	620.507
83	−0.050	0.060	187.2	−19.82	494.081	2358.990	477.518	77.918	630.726
84 *	−0.050	0.065	186.8	−19.83	492.336	2350.660	480.521	80.498	639.783
85	−0.050	0.070	186.4	−19.84	475.930	2272.328	469.145	80.638	629.620
86	−0.050	0.075	186.0	−19.85	465.163	2220.918	463.166	81.636	626.530
87	−0.050	0.080	185.6	−19.86	473.326	2259.893	476.121	86.008	649.140
88	−0.050	0.085	185.2	−19.87	464.431	2217.427	472.021	87.343	648.607
89	−0.050	0.090	184.8	−19.88	453.291	2164.238	465.543	88.198	644.705
90	−0.050	0.095	184.4	−19.89	448.079	2139.356	465.094	90.169	649.094
91	−0.050	0.100	184.0	−19.90	444.772	2123.565	466.648	92.540	656.302
92	−0.045	0.080	184.2	−19.93	445.038	2124.835	467.741	91.481	658.338
93	−0.040	0.060	184.4	−19.96	450.533	2151.072	474.345	91.476	668.139
94	−0.035	0.040	184.6	−19.99	438.784	2094.975	462.786	87.980	652.351
95	−0.030	0.020	184.8	−20.02	446.968	2134.050	472.249	88.484	666.195
96	−0.025	0.000	185.0	−20.05	435.131	2077.532	460.555	85.028	650.192
97	−0.020	−0.020	185.2	−20.08	443.189	2116.005	469.916	85.464	663.912
98 *	−0.015	−0.040	185.4	−20.11	428.283	2044.835	454.919	81.482	643.213
99	−0.010	−0.060	185.6	−20.14	443.389	2116.960	471.807	83.205	667.598
100	−0.005	−0.080	185.8	−20.17	435.256	2078.129	463.983	80.542	657.028
101	0.000	−0.100	186.0	−20.20	433.272	2068.658	462.699	79.037	655.711
102	0.000	−0.095	186.1	−20.16	438.555	2093.882	458.243	79.003	652.932
103	0.000	−0.090	186.2	−20.12	446.871	2133.586	456.984	79.518	654.697
104	0.000	−0.085	186.3	−20.08	448.202	2139.939	448.691	78.800	646.346
105	0.000	−0.080	186.4	−20.04	462.791	2209.595	453.648	80.412	657.090
106	0.000	−0.075	186.5	−20.00	465.942	2224.642	447.330	80.030	651.527
107	0.000	−0.070	186.6	−19.96	473.533	2260.882	445.353	80.418	652.256
108	0.000	−0.065	186.7	−19.92	477.424	2279.462	439.958	80.184	647.954
109	0.000	−0.060	186.8	−19.88	485.096	2316.091	438.105	80.591	648.845
110 *	0.000	−0.055	186.9	−19.84	507.266	2421.943	449.073	83.379	668.839
111	0.000	−0.050	187.0	−19.8	507.444	2422.792	440.439	82.539	659.692
112	0.000	−0.045	187.1	−19.81	502.758	2400.418	443.057	83.043	658.460
113	0.000	−0.040	187.2	−19.82	501.649	2395.121	448.936	84.157	661.993
114	0.000	−0.035	187.3	−19.83	477.620	2280.398	434.147	81.397	635.166
115	0.000	−0.030	187.4	−19.84	485.300	2317.065	448.147	84.035	650.483
116	0.000	−0.025	187.5	−19.85	477.677	2280.670	448.218	84.061	645.435

Table A1. *Cont.*

Number	α_{in}	α_{out}	β_{oil}	α_{oil}	P kW	N Nm	Q kW	P_{mic} bar	T_{mo} K
117	0.000	−0.020	187.6	−19.86	471.945	2253.301	450.073	84.422	642.949
118	0.000	−0.015	187.7	−19.87	450.064	2148.829	436.312	81.853	618.306
119	0.000	−0.010	187.8	−19.88	446.239	2130.566	439.865	82.531	618.330
120	0.000	−0.005	187.9	−19.89	444.939	2124.359	446.048	83.704	621.956
121	0.000	0.000	188.0	−19.90	438.336	2092.835	447.014	83.898	618.242
122 *	0.000	0.005	187.6	−19.91	441.460	2107.748	450.789	85.038	626.993
123	0.000	0.010	187.2	−19.92	429.012	2048.320	438.652	83.168	613.551
124	0.000	0.015	186.8	−19.93	437.432	2088.519	447.848	85.340	629.924
125	0.000	0.020	186.4	−19.94	442.048	2110.558	453.169	86.788	640.962
126	0.000	0.025	186.0	−19.95	436.067	2082.000	447.625	86.155	636.633
127	0.000	0.030	185.6	−19.96	437.838	2090.458	450.036	87.050	643.593
128	0.000	0.035	185.2	−19.97	433.071	2067.699	445.725	86.644	640.926
129	0.000	0.040	184.8	−19.98	437.087	2086.874	450.453	87.995	651.263
130	0.000	0.045	184.4	−19.99	439.796	2099.807	453.845	89.093	659.732
131	0.000	0.050	184.0	−20.00	431.890	2062.058	446.278	88.036	652.239
132	0.000	0.055	184.1	−20.01	432.261	2063.832	447.258	87.894	657.045
133	0.000	0.060	184.2	−20.02	432.100	2063.064	447.686	87.644	661.040
134	0.000	0.065	184.3	−20.03	437.175	2087.291	453.545	88.454	673.088
135 *	0.000	0.070	184.4	−20.04	430.908	2057.369	447.636	86.970	667.659
136	0.000	0.075	184.5	−20.05	441.041	2105.752	458.769	88.795	687.675
137	0.000	0.080	184.6	−20.06	440.570	2103.503	458.883	88.480	691.247
138	0.000	0.085	184.7	−20.07	428.063	2043.787	446.443	85.754	675.803
139	0.000	0.090	184.8	−20.08	429.063	2048.560	448.073	85.740	681.567
140	0.000	0.095	184.9	−20.09	441.691	2108.853	461.865	88.044	705.931
141	0.000	0.100	185.0	−20.10	433.986	2072.067	454.402	86.292	697.843
142	0.005	0.080	185.2	−20.08	433.094	2067.809	453.495	84.840	689.066
143	0.010	0.060	185.4	−20.06	429.127	2048.867	449.368	82.801	675.478
144	0.015	0.040	185.6	−20.04	438.779	2094.952	459.504	83.372	683.230
145	0.020	0.020	185.8	−20.02	429.856	2052.345	450.186	80.412	662.044
146 *	0.025	0.000	186.0	−20.00	432.012	2062.639	452.471	79.543	658.036
147	0.030	−0.020	186.2	−19.98	432.260	2063.823	452.759	78.317	651.080
148	0.035	−0.040	186.4	−19.96	427.376	2040.505	447.671	76.173	636.471
149	0.040	−0.060	186.6	−19.94	433.600	2070.224	454.218	76.006	638.382
150	0.045	−0.080	186.8	−19.92	427.689	2042.001	448.053	73.710	622.419
151	0.050	−0.100	187.0	−19.90	433.639	2070.409	454.314	73.458	623.716
152	0.050	−0.095	187.1	−19.91	434.673	2075.345	454.106	74.465	630.109
153	0.050	−0.090	187.2	−19.92	439.307	2097.469	457.644	76.097	641.778
154	0.050	−0.085	187.3	−19.93	441.766	2109.212	458.897	77.366	650.343
155	0.050	−0.080	187.4	−19.94	428.543	2046.077	443.893	75.866	635.694
156	0.050	−0.075	187.5	−19.95	427.125	2039.308	441.163	76.427	638.386
157	0.050	−0.070	187.6	−19.96	429.764	2051.909	442.621	77.716	647.148
158 *	0.050	−0.065	187.7	−19.97	428.579	2046.251	440.137	78.314	650.162
159	0.050	−0.060	187.8	−19.98	434.792	2075.916	445.239	80.273	664.449
160	0.050	−0.055	187.9	−19.99	439.951	2100.546	449.228	82.058	677.245
161	0.050	−0.050	188.0	−20.00	436.549	2084.302	444.473	82.248	676.876
162	0.050	−0.045	187.6	−20.01	436.311	2083.169	445.624	83.355	674.778
163	0.050	−0.040	187.2	−20.02	446.239	2130.567	457.184	86.425	688.369
164	0.050	−0.035	186.8	−20.03	441.326	2107.113	453.550	86.631	679.053
165	0.050	−0.030	186.4	−20.04	440.192	2101.696	453.776	87.558	675.580
166	0.050	−0.025	186.0	−20.05	437.098	2086.924	451.963	88.081	669.122
167	0.050	−0.020	185.6	−20.06	448.304	2140.429	464.958	91.503	684.530
168	0.050	−0.015	185.2	−20.07	434.778	2075.848	452.290	89.867	662.187
169	0.050	−0.010	184.8	−20.08	450.738	2152.051	470.299	94.329	684.750
170 *	0.050	−0.005	184.4	−20.09	440.920	2105.172	461.425	93.407	668.132
171	0.050	0.000	184.0	−20.10	443.854	2119.180	465.871	95.166	670.871
172	0.050	0.005	184.1	−20.11	441.862	2109.672	468.230	93.229	670.283
173	0.050	0.010	184.2	−20.12	439.624	2098.986	470.354	91.232	669.335
174	0.050	0.015	184.3	−20.13	434.976	2076.791	469.899	88.734	664.716
175	0.050	0.020	184.4	−20.14	435.351	2078.585	474.899	87.252	667.792

Table A1. *Cont.*

Number	α_{in}	α_{out}	β_{oil}	α_{oil}	P kW	N Nm	Q kW	P_{mic} bar	T_{mo} K
176	0.050	0.025	184.5	−20.15	425.565	2031.862	468.787	83.743	655.264
177	0.050	0.030	184.6	−20.16	419.156	2001.263	466.294	80.932	647.882
178	0.050	0.035	184.7	−20.17	421.140	2010.734	473.164	79.733	653.487
179	0.050	0.040	184.8	−20.18	422.307	2016.303	479.227	78.342	657.884
180	0.050	0.045	184.9	−20.19	417.043	1991.172	478.025	75.747	652.281
181	0.050	0.050	185.0	−20.20	409.677	1956.001	474.346	72.792	643.354
182 *	0.050	0.055	185.1	−20.16	422.704	2018.201	474.331	74.228	644.324
183	0.050	0.060	185.2	−20.12	426.643	2037.008	464.304	74.079	631.683
184	0.050	0.065	185.3	−20.08	445.843	2128.680	470.868	76.578	641.615
185	0.050	0.070	185.4	−20.04	448.249	2140.165	459.714	76.194	627.402
186	0.050	0.075	185.5	−20.00	472.337	2255.173	470.685	79.489	643.393
187	0.050	0.080	185.6	−19.96	484.904	2315.175	469.774	80.822	643.173
188	0.050	0.085	185.7	−19.92	481.593	2299.364	453.838	79.529	622.354
189	0.050	0.090	185.8	−19.88	502.060	2397.086	460.455	82.171	632.450
190	0.050	0.095	185.9	−19.84	509.058	2430.499	454.592	82.601	625.415
191	0.050	0.100	186.0	−19.80	522.206	2493.273	454.277	84.033	626.009
192	0.055	0.080	186.2	−19.83	515.216	2459.900	456.973	84.186	633.892
193	0.060	0.060	186.4	−19.86	495.097	2363.842	447.887	82.174	625.371
194 *	0.065	0.040	186.6	−19.89	497.580	2375.697	459.283	83.918	645.462
195	0.070	0.020	186.8	−19.92	489.354	2336.423	461.051	83.893	652.136
196	0.075	0.000	187.0	−19.95	469.128	2239.852	451.336	81.786	642.492
197	0.080	−0.020	187.2	−19.98	457.320	2183.476	449.463	81.109	643.901
198	0.085	−0.040	187.4	−20.01	455.046	2172.618	457.072	82.139	658.939
199	0.090	−0.060	187.6	−20.04	435.982	2081.596	447.766	80.130	649.573
200	0.095	−0.080	187.8	−20.07	429.609	2051.167	451.353	80.434	658.853
201	0.100	−0.100	188.0	−20.10	425.114	2029.706	457.115	81.119	671.388
202	0.100	−0.095	187.6	−20.11	425.553	2031.803	458.094	82.278	679.348
203	0.100	−0.090	187.2	−20.12	428.094	2043.934	461.343	83.859	690.766
204	0.100	−0.085	186.8	−20.13	419.525	2003.024	452.616	83.256	684.205
205	0.100	−0.080	186.4	−20.14	424.794	2028.180	458.817	85.398	700.208
206 *	0.100	−0.075	186.0	−20.15	413.241	1973.021	446.846	84.150	688.425
207	0.100	−0.070	185.6	−20.16	417.281	1992.308	451.729	86.065	702.539
208	0.100	−0.065	185.2	−20.17	418.252	1996.946	453.301	87.369	711.629
209	0.100	−0.060	184.8	−20.18	409.455	1954.945	444.280	86.619	704.013
210	0.100	−0.055	184.4	−20.19	411.802	1966.147	447.345	88.217	715.494
211	0.100	−0.050	184.0	−20.20	410.100	1958.022	446.018	88.958	720.008
212	0.100	−0.045	184.1	−20.16	417.385	1992.804	445.067	87.532	703.968
213	0.100	−0.040	184.2	−20.12	426.837	2037.933	446.519	86.591	691.882
214	0.100	−0.035	184.3	−20.08	435.874	2081.079	447.588	85.583	679.288
215	0.100	−0.030	184.4	−20.04	451.615	2156.238	455.473	85.869	676.921
216	0.100	−0.025	184.5	−20.00	457.493	2184.302	453.400	84.275	659.735
217 *	0.100	−0.020	184.6	−19.96	481.972	2301.173	469.608	86.057	668.876
218	0.100	−0.015	184.7	−19.92	483.110	2306.608	463.001	83.646	645.388
219	0.100	−0.010	184.8	−19.88	488.974	2334.607	461.148	82.129	628.941
220	0.100	−0.005	184.9	−19.84	509.723	2433.673	473.253	83.085	631.383
221	0.100	0.000	185.0	−19.80	516.548	2466.257	472.338	81.741	616.278
222	0.100	0.005	185.1	−19.81	511.380	2441.583	473.848	81.457	617.829
223	0.100	0.010	185.2	−19.82	494.387	2360.451	464.296	79.280	604.965
224	0.100	0.015	185.3	−19.83	504.046	2406.566	479.858	81.384	624.818
225	0.100	0.020	185.4	−19.84	495.208	2364.370	478.002	80.518	621.979
226	0.100	0.025	185.5	−19.85	476.074	2273.013	466.018	77.962	605.973
227	0.100	0.030	185.6	−19.86	481.002	2296.544	477.585	79.346	620.591
228	0.100	0.035	185.7	−19.87	460.046	2196.490	463.417	76.457	601.772
229 *	0.100	0.040	185.8	−19.88	469.805	2243.085	480.232	78.676	623.181
230	0.100	0.045	185.9	−19.89	455.612	2175.321	472.703	76.897	612.992
231	0.100	0.050	186.0	−19.90	447.409	2136.156	471.257	76.117	610.700
232	0.100	0.055	186.1	−19.91	451.170	2154.112	476.258	77.807	623.612
233	0.100	0.060	186.2	−19.92	437.730	2089.940	463.092	76.523	612.683
234	0.100	0.065	186.3	−19.93	435.036	2077.077	461.272	77.093	616.617

Table A1. *Cont.*

Number	α_{in}	α_{out}	β_{oil}	α_{oil}	P kW	N Nm	Q kW	P_{mic} bar	T_{mo} K
235	0.100	0.070	186.4	−19.94	436.906	2086.006	464.303	78.484	627.111
236	0.100	0.075	186.5	−19.95	438.642	2094.295	467.215	79.874	637.585
237	0.100	0.080	186.6	−19.96	421.193	2010.988	449.669	77.747	619.994
238 *	0.100	0.085	186.7	−19.97	418.885	1999.968	448.252	78.380	624.433
239	0.100	0.090	186.8	−19.98	432.048	2062.814	463.433	81.950	652.251
240	0.100	0.095	186.9	−19.99	428.435	2045.561	460.659	82.378	655.037
241	0.100	0.100	187.0	−20.00	417.703	1994.322	450.209	81.416	646.779

Note: Superscript * indicates that this sample is the verification data.

References

1. Zhu, Z.; Zhang, F.; Li, C.; Wu, T.; Han, K.; Lv, J.; Li, Y.; Xiao, X. Genetic algorithm optimization applied to the fuel supply parameters of diesel engines working at plateau. *Appl. Energy* **2015**, *157*, 789–797. [CrossRef]
2. Huaiqing, Z. Research on Power Enhancement of 16V280ZJA Diesel Engine for Plateau Locomotive. Master's Thesis, Shanghai Jiaotong University, Shanghai, China, 2007.
3. Qiangqiang, T.; Deyuan, W.; Chengguan, W.; Yuan, L.; Diming, L.; Yunguang, L.; Sheng, L.; Zhenhuan, Y. Research on Performance Optimization of Heavy-duty Diesel Engines in Plateau Environment. *Ordnance Ind.* **2018**, *39*, 436–443.
4. Zhang, H.; Zhang, H.; Wang, Z. Effect on Vehicle Turbocharger Exhaust Gas Energy Utilization for the Performance of Centrifugal Compressors under Plateau Conditions. *Energies* **2017**, *10*, 2121. [CrossRef]
5. Xia, M.; Zhao, C.; Zhang, F.; Huang, Y. Modeling the Performance of a New Speed Adjustable Compound Supercharging Diesel Engine Working under Plateau Conditions. *Energies* **2017**, *10*, 689.
6. Qiao, Y.; Lyu, G.; Song, C.; Liang, X.; Zhang, H.; Dong, D. Optimization of Programmed Temperature Vaporization Injection for Determination of Polycyclic Aromatic Hydrocarbons from Diesel Combustion Process. *Energies* **2019**, *12*, 4791. [CrossRef]
7. Cococcetta, F.; Finesso, R.; Hardy, G.; Marello, O.; Spessa, E. Implementation and Assessment of a Model-Based Controller of Torque and Nitrogen Oxide Emissions in an 11 L Heavy-Duty Diesel Engine. *Energies* **2019**, *12*, 4704. [CrossRef]
8. Markov, V.; Kamaltdinov, V.; Zherdev, A.; Furman, V.; Sa, B.; Neverov, V. Study on the Possibility of Improving the Environmental Performance of Diesel Engine Using Carbon Nanotubes as a Petroleum Diesel Fuel Additive. *Energies* **2019**, *12*, 4345. [CrossRef]
9. Nand Agrawal, B.; Sinha, S.; Bandhu Singh, D.; Bansal, G. Effects of blends of castor oil with pure diesel on performance parameters of direct injection compression ignition engine. *Mater. Today Proc.* **2019**, in press. [CrossRef]
10. d'Ambrosio, S.; Ferrari, A.; Mancarella, A.; Mancò, S.; Mittica, A. Comparison of the Emissions, Noise, and Fuel Consumption Comparison of Direct and Indirect Piezoelectric and Solenoid Injectors in a Low-Compression-Ratio Diesel Engine. *Energies* **2019**, *12*, 4023. [CrossRef]
11. Wong, K.I.; Wong, P.K.; Cheung, C.S.; Vong, C.M. Modeling and optimization of biodiesel engine performance using advanced machine learning methods. *Energy* **2013**, *55*, 519–528. [CrossRef]
12. Zhao, J.; Xu, M. Fuel economy optimization of an Atkinson cycle engine using genetic algorithm. *Appl. Energy* **2013**, *105*, 335–348. [CrossRef]
13. Yoo, H.; Park, B.Y.; Cho, H.; Park, J. Performance Optimization of a Diesel Engine with a Two-Stage Turbocharging System and Dual-Loop EGR Using Multi-Objective Pareto Optimization Based on Diesel Cycle Simulation. *Energies* **2019**, *12*, 4223. [CrossRef]
14. Bietresato, M.; Caligiuri, C.; Bolla, A.; Renzi, M.; Mazzetto, F. Proposal of a Predictive Mixed Experimental-Numerical Approach for Assessing the Performance of Farm Tractor Engines Fuelled with Diesel-Biodiesel-Bioethanol Blends. *Energies* **2019**, *12*, 2287. [CrossRef]
15. Najafi, B.; Faizollahzadeh Ardabili, S.; Mosavi, A.; Shamshirband, S.; Rabczuk, T. An Intelligent Artificial Neural Network-Response Surface Methodology Method for Accessing the Optimum Biodiesel and Diesel Fuel Blending Conditions in a Diesel Engine from the Viewpoint of Exergy and Energy Analysis. *Energies* **2018**, *11*, 860. [CrossRef]

16. Li, Z.; Li, Y.; Li, Y. Performance Evaluation of Energy Transition Based on the Technique for Order Preference by a Similar to Ideal Solution and Support Vector Machine Optimized by an Improved Artificial Bee Colony Algorithm. *Energies* **2019**, *12*, 3059. [CrossRef]
17. García Álvarez, J.; González, M.Á.; Rodríguez Vela, C.; Varela, R. Electric Vehicle Charging Scheduling by an Enhanced Artificial Bee Colony Algorithm. *Energies* **2018**, *11*, 2752. [CrossRef]
18. Tan, S.; Wang, X.; Jiang, C. Privacy-Preserving Energy Scheduling for ESCOs Based on Energy Blockchain Network. *Energies* **2019**, *12*, 1530. [CrossRef]
19. Jamaluddin, K.; Wan Alwi, S.R.; Abdul Manan, Z.; Hamzah, K.; Klemeš, J.J. A Process Integration Method for Total Site Cooling, Heating and Power Optimisation with Trigeneration Systems. *Energies* **2019**, *12*, 1030. [CrossRef]
20. Marti-Puig, P.; Blanco-M, A.; Cárdenas, J.J.; Cusidó, J.; Solé-Casals, J. Feature Selection Algorithms for Wind Turbine Failure Prediction. *Energies* **2019**, *12*, 453. [CrossRef]
21. Jiao, Y.; Liu, R.; Zhang, Z.; Yang, C.; Zhou, G.; Dong, S.; Liu, W. Comparison of combustion and emission characteristics of a diesel engine fueled with diesel and methanol-Fischer-Tropsch diesel-biodiesel-diesel blends at various altitudes. *Fuel* **2019**, *243*, 52–59. [CrossRef]
22. Kan, Z.; Hu, Z.; Lou, D.; Tan, P.; Cao, Z.; Yang, Z. Effects of altitude on combustion and ignition characteristics of speed-up period during cold start in a diesel engine. *Energy* **2018**, *150*, 164–175. [CrossRef]
23. Li, M.; Lu, S.; Chen, R.; Guo, J.; Wang, C. Experimental investigation on flame spread over diesel fuel near sea level and at high altitude. *Fuel* **2016**, *184*, 665–671. [CrossRef]
24. Karataş, A.E.; Gülder, Ö.L. Soot formation in high pressure laminar diffusion flames. *Prog. Energy Combust. Sci.* **2012**, *38*, 818–845. [CrossRef]
25. Zhou, Y.; Huang, X.; Peng, S.; Li, L. Comparative study on the combustion characteristics of an atmospheric induction stove in the plateau and plain regions of China. *Appl. Therm. Eng.* **2017**, *111*, 301–307. [CrossRef]
26. El Shenawy, E.A.; Elkelawy, M.; Bastawissi, H.A.-E.; Panchal, H.; Shams, M.M. Comparative study of the combustion, performance, and emission characteristics of a direct injection diesel engine with a partially premixed lean charge compression ignition diesel engines. *Fuel* **2019**, *249*, 277–285. [CrossRef]
27. Giraldo, M.; Huertas, J.I. Real emissions, driving patterns and fuel consumption of in-use diesel buses operating at high altitude. *Transp. Res. Part D Transp. Environ.* **2019**, *77*, 21–36. [CrossRef]
28. Zhang, H.; Shi, L.; Deng, K.; Liu, S.; Yang, Z. Experiment investigation on the performance and regulation rule of two-stage turbocharged diesel engine for various altitudes operation. *Energy* **2020**, *192*, 116653. [CrossRef]
29. Yang, M.; Gu, Y.; Deng, K.; Yang, Z.; Zhang, Y. Analysis on altitude adaptability of turbocharging systems for a heavy-duty diesel engine. *Appl. Therm. Eng.* **2018**, *128*, 1196–1207. [CrossRef]
30. Wang, X.; Guo, M.; He, M.; Gu, C.; Cheng, J. Study on improvement of high power diesel engine performance in plateau environment. *Chin. Intern. Combust. Engine Eng.* **2014**, *35*, 113–118. (In Chinese)
31. Xin, Q. *Diesel Engine System Design*; Elsevier: Amsterdam, The Netherlands, 2011.
32. Menezes, M.V.F.; Torres, L.C.B.; Braga, A.P. Width optimization of RBF kernels for binary classification of support vector machines: A density estimation-based approach. *Pattern Recognit. Lett.* **2019**, *128*, 1–7. [CrossRef]
33. Zhu, Z.X.; Zhang, F.J.; Li, C.J.; Han, K. Calibration for Fuel Injection Parameters of the Diesel Engine Working at Plateau via Simulating. *Adv. Mech. Eng.* **2015**, *6*, 621946. [CrossRef]
34. Belgiorno, G.; Di Blasio, G.; Beatrice, C. Parametric study and optimization of the main engine calibration parameters and compression ratio of a methane-diesel dual fuel engine. *Fuel* **2018**, *222*, 821–840. [CrossRef]